(which would be squared in the three-dimensional (3-D) case, [4]–[6]), there is a very satisfactory agreement.

III. Conclusion

The minimum number of bistatic near field measurements required to evaluate the monostatic RCS of an arbitrary scatterer has been rigorously determined with reference to a 2-D geometry and TM polarization, and an efficient procedure for the evaluation of the monostatic RCS from near-field bistatic RCS measurements has been presented. In particular, it is shown that the evaluation of the monostatic RCS requires the measurement of the near-field bistatic RCS only in a limited angular region, whose extension depends on the dimension of the scattering object and on the distance of the measurement surface from the object. This result allows to reduce both the measurement time and the computational effort to evaluate the monostatic RCS from near-field measurements. Furthermore, the adoption of a numerically effective algorithm for the near-field far-field transformation based on the FFT allows a fast and efficient computation of the monostatic RCS.

In this paper a 2-D geometry has been considered. However, the method can be extended to the 3-D case by following a similar approach developed for 3-D near-field measurements by scanning on a sphere about the object under test, expanding the field in spherical harmonics, and exploiting a covolutional product for the azimuth portion of the transformation [6]. This extension will be the subject of a forthcoming paper.

References

[1] M. Dinallo, "Extension of plane-wave scattering matrix theory of antenna-antenna interaction to three antennas: A near-field radar cross section concept," in *Proc. AMTA*, Oct. 1984.

[2] D. G. Falconer, "Extrapolation of near-field RCS measurements to the far zone," *IEEE Trans. Antennas Propag.*, vol. AP-36, no. 6, pp. 822–829, Jun. 1988.

[3] B. J. Cown and C. E. Ryan Jr., "Near-field scattering measurements for determining complex target RCS," *IEEE Trans. Antennas Propag.*, vol. AP-37, no. 5, pp. 576–585, May 1989.

[4] J. W. Burns and I. J. LaHaie, "Investigation of the minimum sample region required to predict RCS from planar scan near field data," in *URSI Radio Science Meeting Dig.*, Syracuse, NY, 1988, p. 330.

[5] ——, "Algorithm for determing waterline rcs of a high aspect target using SNFFT," in *URSI Radio Science Meeting Dig.*, Seattle, WA, 1994, p. 106.

[6] M. A. Ricoy, "Convolutional form for predicting far zone bistatic RCS from spherical near field measurements," in *PIERS* Seattle, WA, 1995, p. 577.

[7] D. S. Jones, *The Theory of Electromagnetism*. New York: Pergamon Press, 1964.

[8] O. M. Bucci and G. Franceschetti, "On the spatial bandwidth of scattered fields," *IEEE Trans. Antennas Propag.*, vol. AP-35, pp. 1445–1455, 1987.

[9] O. M. Bucci and T. Isernia, "Electromagnetic inverse scattering: Retrievable information and measurement strategies," *Radio Sci.*, vol. 32, no. 4, pp. 2123–2137, Nov.–Dec. 1997.

[10] *Handbook of Mathematical Functions*, Dover, New York, 1970. M. Abramovitz, I. Stegun.

Plane-Wave Diffraction at a Periodically Corrugated Interface Between an Isotropic Medium and a Gyroelectromagnetic Uniaxial Medium

Miriam L. Gigli, Marina E. Inchaussandague, and Ricardo A. Depine

***Abstract*—A formulation of the Rayleigh method for modeling unidimensional periodically corrugated gyroelectromagnetic uniaxial gratings with shallow grooves is presented. The orientation of the preferred axis of the anisotropic medium is arbitrary and incidences from both media are considered. We show that the present method gives reliable results for groove height to period ratio up to 0.3. Numerical examples for sinusoidal gratings in classical and conical mountings are provided.**

***Index Terms*—Anisotropy, gratings, gyroelectromagnetic media, uniaxial crystals.**

I. Introduction

At present, different anisotropic materials are widely used in optics and engineering devices, whether as substrates, films or material fillings [1]–[3]. The interest in surface-relief gratings made of anisotropic materials has grown in the last decade, mainly due to both a natural progression of the electromagnetic theory of gratings and real-world application requirements [4]. However, most of the investigations on anisotropic surface- relief gratings have been limited to media with dielectric anisotropy, that is, media for which the magnetic permeability can be assumed to be that of the vacuum everywhere.

In this paper we investigate the diffraction of electromagnetic waves from gratings made of materials that have uniaxial dielectric and magnetic properties. The preferred axis, the same for both the permeability and the permittivity tensors, is arbitrarily oriented with respect to the grating surface. To the authors knowledge, gyroelectromagnetic uniaxial gratings have been previously analyzed in two particular cases. One, using the T-matrix formalism, when the preferred axis of the anisotropic medium is parallel to the mean surface of the periodic interface and the incident electromagnetic wave in a direction perpendicular to the grating grooves [5]. The other, using a Rayleigh method, for a perfectly matched layer with a shallow corrugation [6]. The primary contribution of this paper is to reformulate and extend previous work [5], [6] to the general case in which: a) the plane of incidence is not perpendicular to the grating grooves (conical diffraction) and b) the optical axis of the general uniaxial material has an arbitrary orientation. To do so, we develop a Rayleigh method to calculate the diffracted fields. This method is based on the assumption that the electromagnetic fields in the region between the grooves can be written as plane-wave expansions [7]. Although not rigorous, Rayleigh methods have proven to give very good results for corrugated isotropic [8], and dielectric anisotropic [9], [10] gratings, even for groove height-to-period ratios greater than 0.14, the limit of validity of the hypothesis for perfect conductors with sinusoidal corrugation.

Manuscript received March 24, 2004; revised January 25, 2005. This work was supported in part by the Consejo Nacional de Investigaciones Científicas y Técnicas (CONICET) and in part by the Agencia Nacional de Promoción Científica y Tecnológica under Contract ANPCYT-BID 802/OC-AR03-04457.

The authors are with the Consejo Nacional de Investigaciones Científicas y Técnicas, Rivadavia 1917, Buenos Aires, Argentina and also with the Grupo de Electromagnetismo Aplicado, Departamento de Física, Facultad de Ciencias Exactas y Naturales, Universidad de Buenos Aires, Ciudad Universitaria, 1428 Buenos Aires, Argentina.

Digital Object Identifier 10.1109/TAP.2005.863146

II. Theory

We consider a periodically corrugated boundary between an isotropic medium and a gyroelectromagnetic uniaxial material. In a rectangular coordinate system (x, y, z) the one-dimensional corrugated boundary is given by the periodic function $y = g(x) = g(x+d)$ (d the period). The grooves of the grating are along the z axis and the y axis is perpendicular to mean surface of the grating, pointing toward the isotropic medium. The plane of incidence forms an angle φ with the main section of the grating ($x - y$ plane). Harmonic time dependence $\exp(-i\,\omega\,t)$ is assumed throughout the paper; in what follows this factor will be omitted.

A. Isotropic Medium

As it is well known, the fields outside the grooves ($y > \max g(x)$) can be rigorously represented by means of Rayleigh expansions

$$\begin{aligned}\vec{E}_1 = &\sum_{n=-\infty}^{+\infty}\left[\frac{-k_z^i\alpha_n R_n^+ + k_0\mu_1\beta_n S_n^+}{\eta}\hat{x}\right.\\ &\left.+\frac{k_z^i\beta_n R_n^+ + k_0\mu_1\alpha_n S_n^+}{\eta}\hat{y} + R_n^+\hat{z}\right]\exp\left(i\vec{k}_{\text{in}}^{+}\cdot\vec{r}\right)\\ &+\sum_{n=-\infty}^{+\infty}\left[\frac{-k_z^i\alpha_n R_n^- - k_0\mu_1\beta_n S_n^-}{\eta}\hat{x}\right.\\ &\left.-\frac{k_z^i\beta_n R_n^- - k_0\mu_1\alpha_n S_n^-}{\eta}\hat{y} + R_n^-\hat{z}\right]\exp\left(i\vec{k}_{\text{in}}^{-}\cdot\vec{r}\right)\end{aligned}\quad(1)$$

where superscript $+(-)$ corresponds to the incident (diffracted) fields, $\vec{r} = x\hat{x} + y\hat{y} + z\hat{z}, k_0$ is the wave number in free space, $R_n^{\pm}$ and $S_n^{\pm}$ are complex amplitudes and $\vec{k}_{\text{in}}^{\pm} = \alpha_n\hat{x} \mp \beta_n\hat{y} + k_z^i\hat{z}, \alpha_n = \alpha_0 + 2\pi n/d, \beta_n = (k_0^2\mu_1\epsilon_1 - \alpha_n^2 - k_z^{i2})^{1/2}$, and $\eta = k_0^2\mu_1\epsilon_1 - k_z^{i2}$.

In the expressions above, ϵ_1 and μ_1 are the permittivity and the permeability of the dielectric medium, respectively. α_0 and k_z^i depend on how the grating is illuminated. For a single plane wave incident onto the grating, we have $\alpha_0 = \Gamma\sin\theta\cos\varphi, k_z^i = \Gamma\sin\theta\sin\varphi$, where θ is the angle between the incident wave vector and the y axis. Γ is given by $\Gamma = k_0(\mu_1\epsilon_1)^{1/2}$, for a wave incident from the isotropic side. On the other hand, when the grating is illuminated from the gyroelectromagnetic medium, the value of Γ is determined from the dispersion equation. In this case, there are two possible values of Γ, which correspond to an incident wave of the electric or magnetic type, respectively.

B. Gyroelectromagnetic Uniaxial Medium

The medium below the interface is a gyroelectromagnetic uniaxial dielectric characterized by permittivity and permeability tensors $\tilde{\epsilon} = \epsilon_\perp\tilde{I} + (\epsilon_\parallel - \epsilon_\perp)\hat{c}\hat{c}$ and $\tilde{\mu} = \mu_\perp\tilde{I} + (\mu_\parallel - \mu_\perp)\hat{c}\hat{c}$ respectively, with $\hat{c} = (c_x, c_y, c_z)$ the optic axis.

In the gyroelectromagnetic uniaxial medium, the total fields in the region below the grating grooves ($y < \min g(x)$) can also be rigorously represented by Rayleigh expansions, now in terms of electric type (subscript 1) and magnetic type (subscript 2) plane waves

$$\begin{aligned}\vec{E}_2 = &\sum_{n=-\infty}^{+\infty}\left[C_{1n}^+\vec{e}_{1n}^{+}\exp\left(i\vec{k}_{1n}^{+}\cdot\vec{r}\right) + C_{2n}^+\vec{e}_{2n}^{+}\exp\left(i\vec{k}_{2n}^{+}\cdot\vec{r}\right)\right]\\ &+\sum_{n=-\infty}^{+\infty}\left[C_{1n}^-\vec{e}_{1n}^{-}\exp\left(i\vec{k}_{1n}^{-}\cdot\vec{r}\right) + C_{2n}^-\vec{e}_{2n}^{-}\exp\left(i\vec{k}_{2n}^{-}\cdot\vec{r}\right)\right]\end{aligned}\quad(2)$$

In the expressions above, the superscript $+(-)$ corresponds to the incident (diffracted) fields. $\vec{k}_{jn}^{\pm} = \alpha_n\hat{x} + \gamma_{jn}^{\pm}\hat{y} + k_z^i\hat{z}(j = 1, 2)$ are the wavenumbers associated with the electric and magnetic waves; they are solutions of the dispersion equations: $\vec{k}_{1n}^{\pm}\cdot\tilde{\epsilon}\cdot\vec{k}_{1n}^{\pm} = k_0^2\mu_\perp\epsilon_\perp\epsilon_\parallel$ and $\vec{k}_{2n}^{\pm}\cdot\tilde{\mu}\cdot\vec{k}_{2n}^{\pm} = k_0^2\mu_\perp\epsilon_\perp\mu_\parallel$. $\vec{e}_{jn}^{\pm}(j = 1, 2)$ are normalized electric field vectors that specify the polarization of the electric ($j = 1$) and magnetic ($j = 2$) waves and $\vec{h}_{jn}^{\pm}(j = 1, 2)$ are related to $\vec{e}_{jn}^{\pm}(j = 1, 2)$ according to Maxwell equations [11]. C_{1n}^- and C_{2n}^- are the unknown complex amplitudes of the fields diffracted into the crystal.

C. Determination of the Fields Using Rayleigh Hypothesis

The boundary conditions require the continuity of the tangential components of $\vec{E}$ and $\vec{H}$ at $y = g(x)$. At this stage we invoke the Rayleigh hypothesis, that is, we assume that expansions (1) and (2), strictly valid outside the grooves, can be replaced into the boundary conditions. Doing so, and then projecting into the Rayleigh basis $\exp(i\alpha_m x)_{m=-\infty}^{+\infty}$, we obtain a system of linear equations, with the amplitudes $C_{1n}^-, C_{2n}^-, R_n^-$, and S_n^- as unknowns [9], [10]. The amplitudes denoted with superscript $+$ are known and specify the polarization of the incident fields. For incident waves from the isotropic side, R_n^+ and S_n^+ are the amplitudes of the z components of the incident electric and magnetic field respectively. These amplitudes can be expressed in terms of the s and p polarization amplitudes of the incident electric field.

When the incidence is from the anisotropic side, we have $C_{1n}^+ = \delta_{n,0}$, and $C_{2n}^+ = 0$ for an incident wave of the electric type or $C_{2n}^+ = \delta_{n,0}$, and $C_{1n}^+ = 0$ when the incident wave is of the magnetic type. The system of equations can be written in matrix form as

$$\begin{bmatrix} M_{11}^- & M_{12}^- & M_{13}^- & M_{14}^- \\ M_{21}^- & M_{22}^- & M_{23}^- & M_{24}^- \\ M_{31}^- & M_{32}^- & M_{33}^- & M_{34}^- \\ M_{41}^- & M_{42}^- & M_{43}^- & M_{44}^- \end{bmatrix}\begin{bmatrix} R_n^- \\ S_n^- \\ C_{1n}^- \\ C_{2n}^- \end{bmatrix} = \begin{bmatrix} M_{11}^+ & M_{12}^+ & M_{13}^+ & M_{14}^+ \\ M_{21}^+ & M_{22}^+ & M_{23}^+ & M_{24}^+ \\ M_{31}^+ & M_{32}^+ & M_{33}^+ & M_{34}^+ \\ M_{41}^+ & M_{42}^+ & M_{43}^+ & M_{44}^+ \end{bmatrix}\begin{bmatrix} R_n^+ \\ S_n^+ \\ C_{1n}^+ \\ C_{2n}^+ \end{bmatrix}\quad(3)$$

where

$$\begin{aligned}M_{11}^{\pm}|_{mn} &= \mp D_{mn}(\mp\beta_n) = M_{32}^{\pm}|_{mn}, M_{12}^{\pm}|_{mn}\\ &= M_{31}^{\pm}|_{mn} = 0,\end{aligned}\quad(4)$$

$$\begin{aligned}M_{13}^{\pm}|_{mn} &= \pm\left(\vec{e}_{1n}^{\pm}\cdot\hat{z}\right)D_{mn}\left(\gamma_{1n}^{\pm}\right)M_{33}^{\pm}|_{mn}\\ &= \pm\left(\vec{h}_{1n}^{\pm}\cdot\hat{z}\right)D_{mn}\left(\gamma_{1n}^{\pm}\right)\end{aligned}\quad(5)$$

$$M_{21}^{\pm}|_{mn} = \frac{k_z^i}{\eta}[\beta_n E_{mn}(\mp\beta_n) \mp \alpha_n D_{mn}(\mp\beta_n)] = M_{42}^{\pm}|_{mn}\quad(6)$$

$$M_{22}^{\pm}|_{mn} = \frac{\omega\mu_1}{c\eta}[\pm\alpha_n E_{mn}(\mp\beta_n) + \beta_n D_{mn}(\mp\beta_n)]\quad(7)$$

$$M_{23}^{\pm}|_{mn} = \mp\left(\vec{e}_{1n}^{\pm}\cdot\hat{y}\right)E_{mn}\left(\gamma_{1n}^{\pm}\right) \mp \left(\vec{e}_{1n}^{\pm}\cdot\hat{x}\right)D_{mn}(\gamma_{1n}^{\pm})\quad(8)$$

$$M_{41}^{\pm}|_{mn} = \frac{\omega\epsilon_1}{c\eta}[\mp\alpha_n E_{mn}(\mp\beta_n) - \beta_n D_{mn}(\mp\beta_n)]\quad(9)$$

$$M_{43}^{\pm}|_{mn} = \mp\left(\vec{h}_{1n}^{\pm}\cdot\hat{y}\right)E_{mn}(\gamma_{1n}^{\pm}) \mp \left(\vec{h}_{1n}^{\pm}\cdot\hat{x}\right)D_{mn}(\gamma_{1n}^{\pm})\quad(10)$$

$$D_{mn}(u) = \int_0^d \exp\left[i\frac{2\pi}{d}(n-m)x + i\,u\,g(x)\right]dx\quad(11)$$

$$E_{mn}(u) = \int_0^d g'(x)\exp\left[i\frac{2\pi}{d}(n-m)x + i\,u\,g(x)\right]dx\quad(12)$$

and $M_{14}^{\pm}|_{mn}, M_{24}^{\pm}|_{mn}, M_{34}^{\pm}|_{mn}$, and $M_{44}^{\pm}|_{mn}$ have the same expressions as $M_{13}^{\pm}|_{mn}, M_{23}^{\pm}|_{mn}, M_{33}^{\pm}|_{mn}$, and $M_{43}^{\pm}|_{mn}$, respectively, but replacing subscript 1 by 2.

Once we have determined the unknown amplitudes, the efficiencies of the diffracted orders can be calculated. The efficiency of the nth

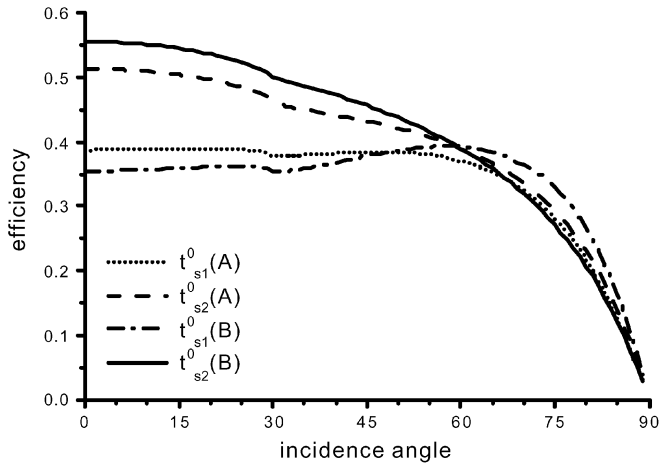

Fig. 1. Efficiency of the zeroth transmitted order of the electric (t^0_{s1}) and of the magnetic type (t^0_{s2}) as a function of the angle of incidence. The polarization of the incident wave is TE, $\mu_\perp = 1.2, \mu_\parallel = 1.05, \lambda/d = 0.5, \varphi_c = 40°$, and $\theta_c = 90°$. Case (A): $\epsilon_\perp = 2.5, \epsilon_\parallel = 1.8$; case (B): $\epsilon_\perp = 1.8, \epsilon_\parallel = 2.5$.

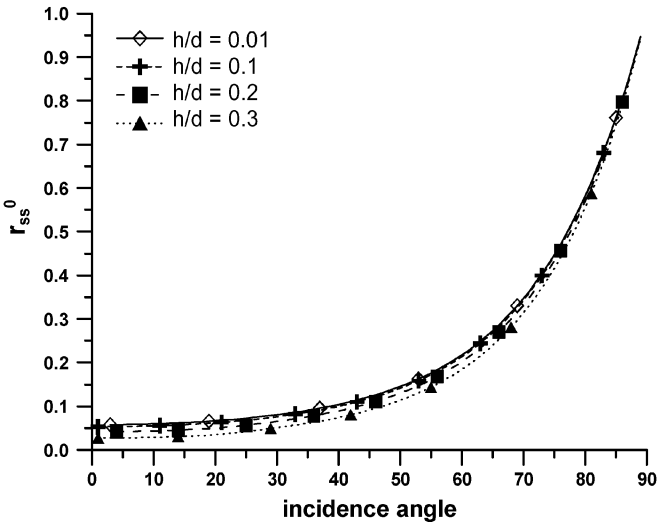

Fig. 2. Zeroth order co-polarized efficiency r^0_{ss} versus angle of incidence θ for a sinusoidal profile with different values of h/d. Other parameters are $\varphi = 0, \lambda/d = 2, \epsilon_1 = 1, \mu_1 = 1, \epsilon_\perp = 2.75, \epsilon_\parallel = 2.32, \mu_\perp = 1, \mu_\parallel = 0.95, \varphi_c = 45°$ and $\theta_c = 45°$.

diffracted order in the isotropic (gyroelectromagnetic) medium is denoted by $r^n_{lj}(t^n_{lj})$, where the first (second) subscript refers to the incident (diffracted) polarization. Subscript $s(p)$ is used to denote TE (TM) polarization, whereas subscript 1 (2) is used for waves in the gyroelectromagnetic medium of the electric (magnetic) type.

III. Results

The system of (3) can be solved numerically retaining $2N+1$ terms in the expansions of the fields, a procedure that leads to a system of $8N+4$ linear equations with $8N+4$ unknowns: R^-_n, S^-_n, C^-_{1n} and C^-_{2n} with n varying in the range $(-N, N)$. The value of N was selected so that the conservation of energy is satisfied within a tolerance of 10^{-6}. To achieve this goal, we have selected $N = 10$ for our examples (N may vary from $N = 5$ to $N = 15$, depending on the height to period ratio h/d and the wavelength to period ratio λ/d).

To validate our program, we have checked our results for an almost flat interface ($h/d \to 0$) between vacuum and a gyroelectromagnetic uniaxial material with arbitrary orientation of the optic axis. In this case, results obtained with our program are in perfect agreement with those presented in a previous paper by M. Simon *et al.* [12], who have found the reflection and refraction coefficients exclusively for *flat* isotropic—gyroelectromagnetic interfaces.

Secondly, we have considered the case of gyroelectromagnetic gratings with the optic axis in the plane of the interface. In this situation, we have reproduced the curves given in [5] for sinusoidal profiles with $h/d = 0.1$ for a grating with the optic axis in the $x - z$ plane forming an angle $\tau = 40°$ with the x axis. As an example, we plot in Fig. 1, the efficiency of the zeroth transmitted order of the electric (t^0_{s1}) and of the magnetic type (t^0_{s2}) as a function of the angle of incidence with the same parameters used in [5, Fig. 1]. The polarization of the incident wave is TE, $\mu_\perp = 1.2, \mu_\parallel = 1.05, \lambda/d = 0.5$. Case (A): $\epsilon_\perp = 2.5, \epsilon_\parallel = 1.8$; case (B): $\epsilon_\perp = 1.8, \epsilon_\parallel = 2.5$. As it can be observed in this figure, the curves obtained with the present method for a grating with the optic axis in the plane of the interface are identical to those previously obtained in [5].

As examples of the method described above, we investigate the case of sinusoidal profiles given by $g(x) = (h/2)\sin(2\pi x/d)$. We have studied gratings in classical mounting illuminated from the isotropic medium by a plane wave with TE polarization. To study the changes that the corrugation of the interface introduce in the power carried by the diffracted orders, we have considered a grating with the same parameters as in [12] ($\epsilon_e/\epsilon_o = 0.8457, \mu_e/\mu_o = 0.95, \varphi_c = 45°$, and $\theta_c = 45°$). θ_c is the angle between the optic axis and the y axis, and φ_c is the angle between the x axis and the projection of the optic axis onto the $x - y$ plane. In the examples, the value of $\lambda/d = 2$ was selected so as to have only one order reflected in the isotropic medium. Four values of h/d were considered: 0.01, 0.1, 0.2, and 0.3.

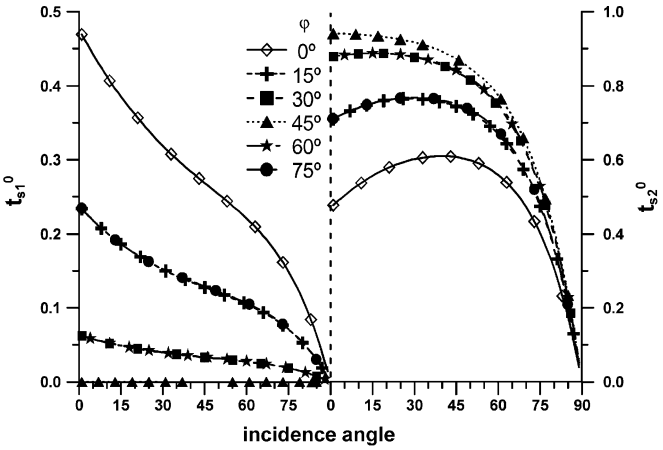

Fig. 3. Efficiencies of the zeroth transmitted orders of the electric type as function of the angle of incidence θ for different values of φ and $h/d = 0.1$. Other parameters are the same as Fig. 2. (a)t^0_{s1} (b) t^0_{s2}.

In Fig. 2 we show curves corresponding to the the co-polarized reflection efficiency of the zeroth reflected order r^0_{ss} as a function of the angle of incidence. As it can be appreciated in this figure, this efficiency is very small except for near grazing incidence, where almost all the incident energy is reflected back to the isotropic medium.

To show the effects of the orientation of the plane of incidence for this grating, we have varied φ while maintaining the orientation of the optic axis fixed. In Fig. 3(a) and (b), we have plotted the efficiencies of the zeroth transmitted order of the electric and magnetic type for TE incidence (t^0_{s1} and t^0_{s2}, respectively), for $0 < \varphi < 75°, h/d = 0.1$ and the same constitutive parameters as in the previous figures. As it can be seen from these curves, these transmitted efficiencies drastically change when φ is varied; for example, it is observed that efficiency t^0_{s1} at normal incidence, drops approximately from 0.45 for $\varphi = 0°$ to zero for $\varphi = 45°$. Besides, Fig. 3(a) shows that, when the optic axis is

parallel to the plane of incidence ($\varphi = 45^\circ$), t_{s1}^0 vanishes, a result that is related to the polarizations of the fields.

IV. Conclusion

A formulation of the Rayleigh method for calculating the electromagnetic fields scattered by a periodically corrugated interface between an isotropic material and a gyroelectromagnetic uniaxial medium has been presented. The present method can handle general configurations in which the incident beam is associated to waves coming either from the isotropic or from the gyroelectromagnetic side and any orientations with respect to the grooves of the grating for the plane of incidence and for the optical axis of the anisotropic medium. Perfect agreement between the numerical results obtained with this formalism and previous results has been observed for for perfectly flat ($h/d \to 0$) gyroelectromagnetic interfaces and for corrugated gratings in classical mountings with the optic axis of the anisotropic material in the plane of the interface. Results for sinusoidal gratings with different values of h/d in classical and conical mountings were presented.

References

[1] R. E. Collin, *Foundations for Microwave Engineering*, 2nd ed. New York/Piscataway, NJ: Wiley-IEEE Press, 2000.

[2] J. Singh and K. Thyagarajan, "Analysis of metal clad uniaxial waveguides," *Opt. Communications*, vol. 85, pp. 397–402, 1991.

[3] A. Toscano and L. Vegni, "Spectral electromagnetic modeling of a planar integrated structure with a general grounded anisotropic slab," *IEEE Trans. Antennas Propag.*, vol. 41, pp. 362–370, 1993.

[4] L. Li, "Oblique-coordinate-system-based Chandezon method for modeling one-dimensionally periodic, multilayer, inhomogeneous, anisotropic gratings," *J. Opt. Soc. Amer. A*, vol. 16, pp. 2521–2531, 1999.

[5] A. Lakhtakia, R. Depine, M. Inchaussandague, and V. Brudny, "Scattering by a periodically corrugated interface between free space and a gyroelectromagnetic uniaxial medium," *Appl. Opt.*, vol. 32, pp. 2765–2772, 1993.

[6] M. E. Inchaussandague, M. L. Gigli, and R. A. Depine, "Reflection characteristics of a PML with a shallow corrugation," *IEEE Trans. Microw. Theory Techn.*, vol. 51, no. 1691, 2003.

[7] R. Petit, *Electromagnetic Theory of Gratings*, R. Petit, Ed. Heidelberg, Germany: Springer, 1980.

[8] R. Petit, "Plane wave expansions used to describe the field diffracted by a grating," *J. Opt. Soc. Amer.*, vol. 71, pp. 593–598, 1981.

[9] R. A. Depine and M. L. Gigli, "Diffraction from corrugated gratings made with uniaxial crystals: Rayleigh methods," *J. Mod. Opt.*, vol. 41, pp. 695–715, 1994.

[10] R. A. Depine and M. L. Gigli, "Conversion between polarization states at the sinusoidal boundary of a uniaxial crystal," *Phys. Rev. B, Condens. Matter*, vol. 49, pp. 8437–8445, 1994.

[11] H. C. Chen, *Theory of Electromagnetic Waves: A Coordinate Free Approach*. New York: McGraw-Hill, 1983.

[12] M. C. Simon and D. C. Farías, "Reflection and refraction in uniaxial crystals with dielectric and magnetic anisotropy," *J. Mod. Opt.*, vol. 41, pp. 413–429, 1994.

Negative Group Velocity and Anomalous Transmission in a One-Dimensionally Periodic Waveguide

Ruey Bing Hwang

***Abstract*—This study presents a theoretical investigation of the negative group velocity (NGV) and anomalous transmittance of waves in the stop band of a corrugated parallel-plate waveguide (CPPWG). The two different schemes, scattering analysis for a finite CPPWG and the dispersion relation of an infinite CPPWG, were used to investigate the physical insight of the wave process. The NGV zone corresponds to the stopband slanted at an angle on the Brillouin diagram, following the mutual verification of the results obtained by the two different approaches. This class of stopband is caused by the contra-flow interaction between the fundamental mode and the space harmonics of higher-order modes. Additionally, fluctuation was also found in the transmitted coefficient within the conventional stopband, caused by the excitation of the first higher-order mode within the stopband of the fundamental mode.**

***Index Terms*—Corrugated waveguide, negative group velocity, periodic structures.**

I. Introduction

The superluminal group velocity (that is, faster than the speed of light, c, in vacuum) and negative group velocities (NGVs) of the waves in an anomalous dispersion medium have previously been theoretically and experimentally studied [1]–[5]. Recently, Siddiqui, Mojahedi and Eleftheriades [6] designed a new artificial medium having both the Negative Refractive Index and the NGV properties. In their proposed framework, a resonant circuit is embedded within each loaded transmission line unit cell, generating an anomalous dispersion zone with a negative group delay [6]. Besides, dispersion analysis of Sievenpiper's shielded structure using multi-conductor transmission-line theory was carried out and the formation of a *slanted* stopband formed due to contra-directional coupling between the fundamental backward-wave harmonic and the underlying parallel-plate mode was found [7].

In this paper, the NGVs property of the waves guided in a corrugated parallel-plate waveguide (CPPWG) was investigated. The structure under consideration is a parallel-plate waveguide with periodic variation (corrugation) on its bottom wall. Such a CPPWG structure has been widely studied with its guiding characteristics in the pass- and stopbands regions [8]–[12], and has also been employed to design a surface-wave antenna [13]. Here, we took this structure as an example to examine its NGVs property, because that the structure is simple and the mathematical formulation is straightforward. Significantly, dispersion relation of the source-free fields supported by the CPPWG of infinite extent can be exactly predicted.

A rigorous mode-matching method was applied to study such a electromagnetic boundary-values problem consisting of multiple discontinuities. The input-output relation for each discontinuity was first formulated and expressed in terms of the generalized scattering matrix [14]. The scattering characteristics of the overall structure could be obtained by cascading the respective scattering matrix. Besides, the dispersion relation of the infinite periodic structure can be obtained by imposing the Bloch (periodic boundary) condition at the input and output interfaces of a unit cell. The dispersion relation was further converted

Manuscript received April 27, 2005; revised September 9, 2005. This research was supported by National Science Council, Taiwan, R.O.C., under the Contract NSC 94-2213-E-009-069.

The author is with the Department of Communication Engineering National Chiao Tung University, Hsinchu, Taiwan, R.O.C. (e-mail: raybeam@mail.nctu.edu.tw).

Digital Object Identifier 10.1109/TAP.2005.863157